



HAL
open science

SAR imaging of complex environments with EMPRISE ® simulation software

Etienne Everaere, Kévin Unger, Nicolas Trouvé, Flora Weissgerber, Xavier Dupuis, Julien Houssay, Ronan Fabbri, Christian Cochin, Antoine Jouadé

► **To cite this version:**

Etienne Everaere, Kévin Unger, Nicolas Trouvé, Flora Weissgerber, Xavier Dupuis, et al.. SAR imaging of complex environments with EMPRISE ® simulation software. EUSAR 2024, Apr 2024, Munich, Germany. hal-04760342

HAL Id: hal-04760342

<https://hal.science/hal-04760342v1>

Submitted on 30 Oct 2024

HAL is a multi-disciplinary open access archive for the deposit and dissemination of scientific research documents, whether they are published or not. The documents may come from teaching and research institutions in France or abroad, or from public or private research centers.

L'archive ouverte pluridisciplinaire **HAL**, est destinée au dépôt et à la diffusion de documents scientifiques de niveau recherche, publiés ou non, émanant des établissements d'enseignement et de recherche français ou étrangers, des laboratoires publics ou privés.

SAR imaging of complex environments with EMPRISE[®] simulation software

Etienne Everaere^a, Kévin Unger^a, Nicolas Trouvé^a, Flora Weissgerber^b, Xavier Dupuis^c, Julien Houssay^d, Ronan Fabbri^d, Christian Cochin^c, and Antoine Jouadé^e

^aDEMR, ONERA, Université Paris Saclay, F-91123 Palaiseau, France

^bDTIS, ONERA, Université Paris Saclay, F-91123 Palaiseau, France

^cDEMR, ONERA, F-13661 Salon cedex Air, France

^dSCALIAN DS, Rennes, FRANCE

^eDGA-MI, Bruz, FRANCE

Abstract

The development of modern radars relies on digital simulation for their design, evaluation, and qualification. Additionally, simulated SAR data facilitates the development and improvement of processing methods. In this context, ONERA is developing the EMPRISE[®] tool in partnership with SCALIAN-DS, under the supervision of DGA-MI. This paper explains the employed standards, methodologies, and simulation strategies for efficiently simulating radar signals and SAR images of acquisitions over vast real-world terrains and varied environments. A real measurement is compared with the results for our transfer function method and the simulation of the focused complex raw data.

1 Introduction

Various approaches have been used in the literature to simulate SAR images of large and complex scenes. A category of methods proposes to use existing SAR measurements and transform them to create new variations, such as EOSAR [1], where targets are blended into previously acquired images, or the algorithm presented in [2] where new tomographic stacks are derived from real acquisitions. In our case, we are interested in a simulator based on the electromagnetic modelling of a scene in order to control the illumination conditions of the sensor. The study presented in [3] compares two ray-tracing simulators, RaySar [4] and CohRaS [5], with a rasterized rendering-based SAR simulation, SARViz [6]. While these simulators can render simple SAR configurations, none of them simulate the raw signals obtained before SAR synthesis, which is necessary for the development of new sensors. Also, the entire scene needs to be 3D faceted, which is not ideal. The EMPRISE[®] (ElectroMagnetic Product and Radar Image Suite) software package has for main objective to use diverse approaches considering the realism needed for each part of the content of the scene and to produce I/Q signal and SAR image. Major characteristics of SAR image are simulated, such as speckle, layover, shadows, multiple bounces on targets, the electromagnetic response of different materials. The project, funded by DGA (French MoD), has been allocated to ONERA. ONERA is in charge of scientific choices, validation works and production of required data. Number of software developments are done by a dedicated and specialized team of SCALIAN-DS.

In section 2, we present the general principles of the tool as well as the simulation steps. Section 2.1 focuses of the

modeling of the environment and the different steps needed to create a simulation-ready scene. In section 3, two operating modes to produce SAR images, I/Q and "Fast SAR" are described. The Fast SAR mode, uses the convolution of the radar transfer function. Finally, section 4 presents results on large realistic scenes.

2 Simulation approach with EMPRISE[®]

This section describes the simulation strategy and the main steps, which are then described in detail in the following sections. The simulation method involves the first two following concepts :

- Scene models : The scene is composed by geometric and dynamic models as well as an electromagnetic behavior of different kinds of objects and environments. The environment models are chosen pragmatically to be able to compute large scenes while keeping computation times under control.
- Scene discretization : The scene models are called to transform the dynamic objects or environments into elementary scatterers with the computation of their amplitude and phase in the Earth-Centered-Earth-Fixed (ECEF) frame of reference. For each scatterer, a complex amplitude is calculated. It takes into account the reflectivity from the scene model, the phase term introduced by propagation of the wave in the far zone and the amplitude decrease factor inversely proportional to the square of the antenna to scatterer distance.

Phenomena with the greatest impact on radar images are included in the models. For this purpose, different electromagnetic signatures are accepted as input. It includes pre-calculated signatures for objects such as buildings, trees, or even objects derived from a detailed RCS calculation, a sea model and a terrain model. For the creation of input data, we use high-resolution altimetry data such as LiDAR, all while utilizing open geographical data and additional data acquired for the areas to be represented. It is detailed in the following section.

2.1 Scene models

For the moment, the available models are sea, clouds, targets and terrain. The modular approach means that models can be improved, and new models can be added for future developments. Each model provides a dynamic description of scatterers position as well as their reflectivity law depending on illumination condition (incidence, polarisations).

- The marine environment computes EM reflectivity from dynamic sea surface using the GO-SSA model. The dynamic sea model is based on a previous work [7], which was implemented in the MOFREM project [8]. It includes buoyancy and waves generation [9].
- The model for clouds and rain comes from the work presented in [10]. It uses input rain field in format include SSTAR, WRF or HYCELL. The data is divided to voxels elements and converted to volume radar cross section and attenuation for each voxel.
- The terrain model uses a raster representation of the surface without requiring entire 3D model of the scene. Terrain is described in terms of elevation, normals and scene materials. For this purpose the input uses the Common DataBase (CDB) format of OGC [11]. It is organized around several layers with a hierarchy structured, which is perfectly adapted for the Level-Of-Detail (LOD) selection. The model associates each material layer with a parametric or tabulated normalized radar cross-section (σ_0) curve. To calculate the reflectivity of the terrain, the radar resolution cell is oversampled in order to retrieve a proper speckle. The reflectivity model is subject to rigorous validation as presented in [12]. The independent scatterer calculation method reproduces the fully developed speckle with a Rayleigh distribution of scatterer intensities, by coherent summation of the contributions. The model is parameterized by emission and reception polarizations and by the angle of incidence (monostatic). The local angle of incidence is determined using the local normal with the tangent plane approximation. Intensity is derived from the curve of σ_0 of the corresponding material and converted to amplitude using $a = \sqrt{\sigma_0 \cdot S}$, where S is the radar's oversampled resolution cell. Phase is made up of each scatterer self phase φ_0 (0 by default) and the propagation phase $\varphi_p = \frac{4\pi}{\lambda} R_m$ where R_m is the round

trip propagation distance. Finally, in an oversampled radar resolution cell, the amplitude is calculated as the coherent sum of the N scatterers complex amplitudes $p = \frac{1}{\sqrt{N}} \sum_{k=1}^N a_k \cdot e^{i(\varphi_0 + \varphi_p)_k}$. This model enables mixtures of different materials in the same resolution cell.

- Model for above ground objects and moving targets. The 3D objects are pre-computed using MOCEM [13] to form a full signature for every observation angles. The signature is interrogated at compute time to extract the proper scatterers. An object instance gives the proper position, orientation, and scale according to the ground truth.

2.2 Structure of the computation steps

The organization of the sequence of computation steps is similar to a graphical rendering pipeline. The simulator uses GPU computing and implements the pipeline in two modes, the raw data (I/Q) and the Fast SAR mode. The Fast SAR mode only computes the SAR image of an area of the scene considering a SpotLight or StripMap acquisition. The I/Q mode computes the raw data for a custom antenna configuration, which can be multichannel. Additional processing are plugged to the I/Q mode. In this article SAR simulation image in I/Q mode are performed using BackProjection algorithm. The computation strategy can be summarized in the following steps :

- Sequencing: Transcription of the mission of the sensor and the scanning strategy into a list of resulting transmitting and receiving antenna position, sight directions and recording range window for each pulse.
- LOD selection: Selection of the proper level of detail of the models by calculating the resulting resolution cell size on the scene using the scanning strategy and the radar parameters and possible oversampling.
- Batching: Division of the the workload into batches of scenes. The optimization of the calculation pipeline is a key feature of EMPRISE[®]. In the current implementation, the computation can be parallelized for single and multiple GPUs.
- Batch selection: A step preceding the calculation optimizes the selection of calculation batches illuminated by the antennas at each instant. Geometric and radiometric criteria are used to filter the batches for each scene component.
 - The geometric part corresponds to a frustrum culling and uses a factor of the 3dB main lobes of the transmitting and receiving antennas as well as minimum and maximum ranges to define the volume that enclose the scene.
 - The radiometric filtering uses a threshold of the Signal-to-Noise ratio on some position samples in order the keep only area with sufficient level.

- Shadows: The shadow are computed with the Shadow Mapping technique. It enables to compute the mutual shadow of environments and scene objects.
- Computation loop over the time sequence :
 - Fine discretization.
 - Computation of the amplitude and phase of the scatterers.
 - Rasterization.
 - * 1D range grid for the I/Q mode.
 - * 2D range-azimuth grid for the Fast SAR mode.

The rasterization grid is over-sampled in order to retrieve a proper speckle in the final image.

- Convolution of the rasterized grid.
 - * Using the pulse waveform for the I/Q mode.
 - * Using the sensor range-azimuth transfer function for Fast SAR mode.

2.3 Scene creation

Extensive efforts have been dedicated to preparing the scenes for simulation using state-of-the-art remote sensing products, such as topography maps, visible and infrared imaging, and LiDAR data. In France, the National Institute of Geographic and Forest Information (IGN) is a primary source for detailed geographic data. Beyond these foundational resources, there's an emphasis on enhancing the data through specific enrichment processes like photo-based capture and ground truth campaigns. Innovations are also underway to automate these enrichment processes, utilizing either classical techniques or advanced AI methods. Input data undergoes post-processing to form material layers and shapefiles for 3D object instances. One operation involves creating a paved subsurface for housing developments using the cadastre shapefile. This requires creating and refining a shapefile for the housing area, cleaning it by removing road and pavement representations, and then using QGIS tools to differentiate the two shapefiles, thereby isolating paved areas. An example is depicted in Figure 1. Further post-processing includes treating IGN rasters for specific zones using QGIS. Subsequent steps involve re-projecting this raster, cropping, and exporting. Operations in QGIS also facilitate converting linear features into surfaces and separating a shapefile for different objects. The shapefile includes positions parameters, orientations and scale factor. The results are incorporated in the final dataset containing the layers in the CDB format and the shapefiles of above ground objects.

TerrainBuilder is a suite of C++ applications developed by ONERA to performs the conversion from a raster to the CDB format. This suite provides five tools for generating five types of layers : elevation, imagery, materials, Min-MaxElevation, and terrain normals. Operations involve segmenting a raster into smaller tiles. The highest LOD depends on the resolution of original raster. For the subsequent LODs the resolution is reduced iteratively by half through bilinear interpolation.

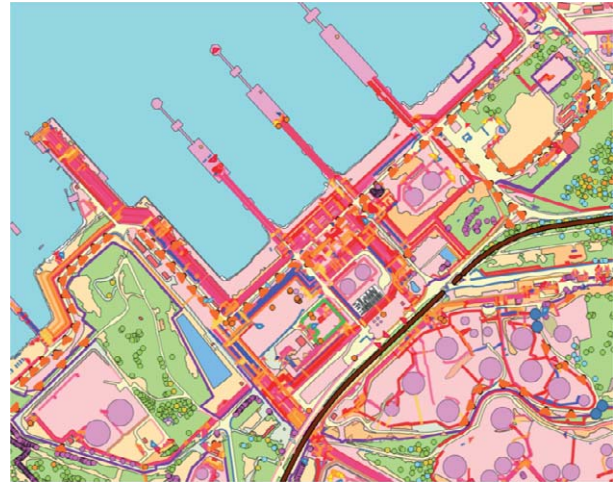


Figure 1 View of the different vector components to create a database, case of Port-de-Bouc harbor.

The resulting data is directly exploited in EMPRISE by the terrain model without necessity of 3D facetization.

3 Synthetic Aperture Radar simulation

3.1 Time domain I/Q

The time domain mode of EMPRISE[®] simulator can be used to compute long integration time along the carrier trajectory for different antenna and channel positions for ether transmission and reception.

Calculation in I/Q mode calculates each transmitted pulse independently. The Start-Stop hypothesis is considered, which freezes the scene during the pulse's round trip. This gives an approximate expression for the round-trip time $\tau(t = k \cdot PRI) = \frac{2 \cdot R_m}{c_0}$, with R_m the round-trip distance from the transmitter position to the scatterer and back to the receiver position, and c_0 the speed of light. Otherwise, we take into account distance ambiguity aliasing and use the temporal method sampled at the pulse repetition frequency to accurately transcribe the scene's dynamics, the carrier's physical and noisy trajectories, and the lever arm effects in antenna positioning. We can select several waveforms, either independently for each pulse or by pulse trains with different coherence groups. Exotic waveforms, such as phase code, can also be used. Advanced SAR modes can be carried out as multi-channel, GMTI, interferometry or altimetry with inclusion of ambiguity phenomenons. A different antenna pointing can be parametrized for each pulse, which enables electronic pointing and AESA antenna logic implementation. The images presented in this article are derived by focusing the raw data with the BPA algorithm.

3.2 Fast SAR mode

The Fast SAR mode (FSM) purpose is to directly produce a SAR image representative of the expected result in the I,Q mode.

FSM is based on the assumption of linear trajectory

with constant velocity with Spotlight or StripMap pointing strategies. The diagram can be taken into account, but for reasons of speed, it is weighted globally in the slant plan rather than by individual contributor. FSM is currently only monostatic, the transmit and receive antennas are co-located and share the same electromagnetic parameters, but will be extended to bistatic in future developments. When the input does not meet this requirement for linear trajectory, an approximated trajectory is calculated and is defined as the tangent line to the real carrier trajectory at the instant corresponding to the middle of the SAR acquisition including the slope influence. This trajectory is used as the azimuth axis of the image frame. The second axis of the image frame correspond to the slant range direction that corresponds to the antenna line of sight. The image frame axis are centered on the carrier antenna phase center at middle acquisition time. The fast SAR image is presented in a geo-referenced slant range/azimuth space and it can easily be projected on a DTM, possibly different from the one used as input, for example to includes uncertainties on the carrier trajectory. The sensor filtering step sub-samples the obtained image to the requested resolution, applies the sensor transfer function and performs zero-padding in azimuth and slant range. The image grid extension in slant range is equal to the swath length. In azimuth, it is equal to the acquisition length for the StripMap case or the azimuth swath for the Spotlight case. The position center of the image grid coincides with the swath position center at the instant corresponding to the middle of the acquisition. An iterative algorithm and the digital elevation model of the terrain are used to geo-reference the image grid corners.

For practical computation considerations, a bounded region of the scene, called the scattering zone, is used to calculate the scattering of the radar waves. The scattering zone is a 3D bounding box and its dimensions are determined thanks to the following procedure. For a given acquisition instant and incidence angle, a quadrilateral can be constructed as the intersection between a plane of constant altitude and a cone with -3dB aperture in distance range and a multiple of -3dB aperture in azimuth range. This construction is done at three acquisition instants (the beginning, middle and end of acquisition) and at two different altitudes (the mean sea level and the altitude of the terrain). The scattering zone is chosen as the minimal bounding box which contains these six quadrilaterals.

3.2.1 The sensor filtering step

The sensor filtering step calculates the fast SAR image from the scatterer complex amplitude grid and takes into account the sensor physical limitations. The scatterer complex amplitude grid is multiplied in the Fourier space with the sensor transfer function related to the azimuth and range resolution required by the user. A scalar factor is applied to the result to take into account the antenna gains at emission and reception. The result grid is sampled down to the resolution cell.

3.2.2 Effects due to moving targets

Some effects due to the movement of targets in the scene are also reproduced, such as delocalisation and defocalisation. Delocalisation is caused by the radial scatterer speed and leads to a shift of the azimuth indices for the corresponding scatterers. Defocalisation is caused by the scatterer azimuth speed or the radial acceleration and leads to a defocalisation factor applied.

To illustrate these effects, we present in Figure 2 a calculation result for the Fast SAR and I/Q configurations for a fishing boat moving at 6m/s in the harbour entrance. The effects of delocalization and focusing are reproduced in both modes, although the spread is finer in the I/Q mode. This also highlights the sea model implemented, which includes the buoyancy of the vessel, and the creation of bow and wake waves.

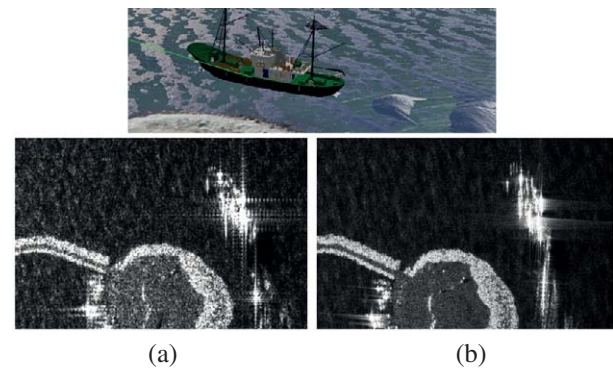


Figure 2 Spotlight view at 0.75m resolution of a fishing boat moving at 7m/s . (a) Fast SAR mode, (b) I/Q mode and BPA focusing.

4 Application examples

This section presents results of scene creation and resulting SAR images for different radar configurations. It demonstrates the capability of EMPRISE[®] to render SAR image of large scene with low computation time.

4.1 Computation of large scenes

The presented results are three area : Port-de-Bouc, Sainte-Marie-la-Mer and Orgon in southern France. Table 1 lists the main features of these databases. Equivalent scene facetization would induces a total number of polygons of the order of 2.10^{10} . The computation time for the entire scene in Fast SAR mode is approximately 10 minutes for a standard workstation, it is compared for each example scene in Table 1.

4.2 Comparison with real measurement

Validation of the entire simulation is an ongoing effort and is beyond the scope of this article. In order to give an overview of the representativeness of the simulation, we compare the simulation results with a measurement performed by ONERA in 2019 using the airborne SAR system SETHI [14]. The configuration is a StripMap mode at

Terrain :	PDB	SMLM	Orgon
Maximum CDB LOD	9	9	11
Area [km^2] :	7	66	63
Number of material classes	24	6	6
Number of object types	26	24	36
Total number of objects instances	16479	454171	615588
Result example	Fig. 3	Fig. 4	Fig. 5
Computation time [s]	82	726	924

Table 1 Main parameter of the example databases. Computation time is given for a workstation with CPU Intel(R) Core(TM) i9 9900X and GPU Nvidia 2080Ti.

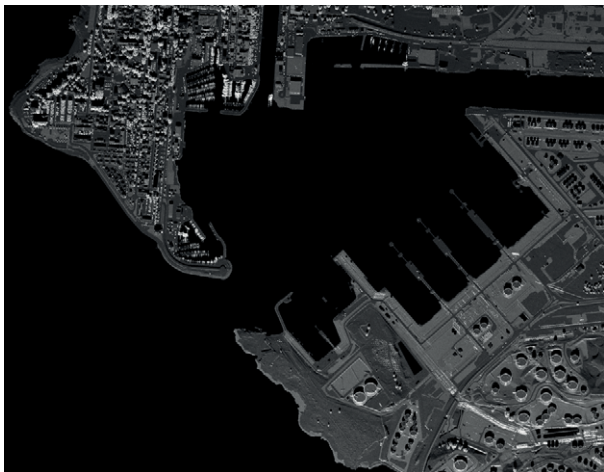


Figure 3 Port-de-Bouc, ships and harbor environments. Fast SAR image of the full area at 3m resolution.



Figure 4 Sainte-Marie-la-Mer town and coastal environments. Fast SAR image of the full area at 3m resolution.

60° incidence angle with 9.75 GHz central frequency, 400 Mhz bandwidth and 0.5 m resolution.

We can distinguish comparisons according to scene components. The main components of the scene are reproduced with the correct positioning, including cultivated fields, roads, vegetation and buildings. The absolute reflectivity level is not open to publication and the σ_0 curves are not recalibrated in this simulation. Nevertheless, the speckle texture is well recovered for the majority of the scene, and the texturing of the terrain height produces visually real-



Figure 5 Orgon, country and forest environments. Fast SAR image of the full area at 3m resolution.

istic behavior. Some parcels of land show lower levels, as the reflectivity curve setting has been underestimated. Some field heights in the database are different when the scene is created and measured, as specific condition can influence the reflectivity as weather or crop height. For pre-calculated and instantiated objects, trees are brighter in the simulation, and work is underway to automate the adjustment of the materials. For buildings and urban areas, the main elements of layover, shading and level are correctly reproduced. The simulation shows fewer strong bright points, such as trihedrons. This can be explained by the limited level of detail of the objects, and also by the smaller number of objects placed in the simulation than in a real scene.

To conclude, this article explains the main structure of EM-PRISE and the strategy of the simulation. Different results examples of SAR image are depicted to give an account of the given possibilities of the tools. Work is underway to improve, enrich and automate the scene creation process, and also to adjust reflectivity curves according to scene materials. Additional work on the polarimetric modes is also currently in progress. Software tools has been developed along with EM-PRISE® to create scenes and simulations for custom study cases. It enables a novice user to familiarize himself with the various radar and SAR techniques and important work is being carried out to provide ergonomic user interfaces for the simulator.

5 Literature

- [1] Sergei Bokaderov, Marcel Laubach, Hartmut Schimpf, and Peter Wellig. Eosar—a tool for the blending of real objects into sar scenes. In *2011 German Microwave Conference*, pages 1–4. IEEE, 2011.
- [2] Mauro Mariotti d’Alessandro and Stefano Tebaldini. Cross sensor simulation of tomographic sar stacks. *Remote Sensing*, 11(18):2099, 2019.
- [3] Timo Balz, Horst Hammer, and Stefan Auer. Potentials and limitations of sar image simulators—a comparative study of three simulation approaches. *ISPRS Journal of photogrammetry and Remote Sensing*, 101:102–109, 2015.
- [4] Stefan Auer, Richard Bamler, and Peter Reinartz. Raysar-3d sar simulator: Now open source. In *2016*



Figure 6 ONERA-DEMRA airborne measurement with the system SETHI over Sainte-Marie-la-Mer area at 0.5m resolution and 60° incidence angle.



Figure 7 EMPRISE simulation of airborne SAR acquisition over Sainte-Marie-la-Mer area at 0.5m resolution and 60° incidence angle.

IEEE International Geoscience and Remote Sensing Symposium (IGARSS), pages 6730–6733. IEEE, 2016.

- [5] Horst Hammer, Silvia Kuny, and Karsten Schulz. Amazing sar imaging effects-explained by sar simulation. In *EUSAR 2014; 10th European Conference on Synthetic Aperture Radar*, pages 1–4. VDE, 2014.
- [6] Timo Balz and Uwe Stilla. Hybrid gpu-based single-and double-bounce sar simulation. *IEEE Transactions on Geoscience and Remote Sensing*, 47(10):3519–3529, 2009.
- [7] Goulven Monnier, Daniel Le Hellard, Sébastien Vince, Thierry Landeau, Bertrand Chapron, René Garello, Gérard Llorç-Pujol, Christian Cochin, and Yvonick Hurtaud. Gpu-based simulation of radar sea clutter.
- [8] Julien Houssay, Nicolas Pinel, Yann-Hervé Hellouvy, Goulven Monnier, Corentin Le Barbu, Christian Cochin, and Yvonick Hurtaud. A physical radar simulation tool of the sea clutter. In *2014 International Radar Conference*, pages 1–6. IEEE, 2014.
- [9] Nicolas Pinel, Goulven Monnier, and Julien Houssay. Fast simulation of a moving sea surface remotely sensed by radar. In *2014 International Radar Conference*, pages 1–6. IEEE, 2014.
- [10] Kourogorgas Charilaos, Féral Laurent, Fabbro Vincent, Jeannin Nicolas, and Lemorton Joël. Use of the hycell model for predicting rain attenuation on uas low elevation datalinks. In *Proceedings of the Fourth European Conference on Antennas and Propagation*, pages 1–5, 2010.
- [11] Sara Saeedi, Steve Liang, David Graham, Michael F Lokuta, and Mir Abolfazl Mostafavi. Overview of the ogc cdb standard for 3d synthetic environment modeling and simulation. *ISPRS International Journal of Geo-Information*, 6(10):306, 2017.
- [12] Flora Weissgerber, Elise Colin, and Nicolas Trouvé. Modeling of the impact of the soil roughness on polsar images. In *EUSAR 2021; 13th European Conference on Synthetic Aperture Radar*, pages 1–6. VDE, 2021.
- [13] Christian Cochin, Philippe Pouligen, Benoit Delahaye, Daniel le Hellard, Philippe Gosselin, and Franck Aubineau. Mocem-an’all in one’tool to simulate sar image. In *7th European Conference on Synthetic Aperture Radar*, pages 1–4. VDE, 2008.
- [14] Jérôme Henrion, Olivier Boisot, Rémi Baqué, Nicolas Castet, Jean-François Nouvel, and Olivier Ruault du Plessis. Sethi : Digital radar system for signal generation and acquisition. In *2019 International Radar Conference (RADAR)*, pages 1–4, 2019.